doi:10.1115/ICEF2018-9618 Pre-Print

Proceedings of the ASME 2018 Internal Combustion Fall Technical Conference
ICEF2018
November 4-7, 2018, San Diego, CA, USA

A COMPUTATIONAL INVESTIGATION OF NON-PREMIXED COMBUSTION OF NATURAL GAS INJECTED INTO MIXTURE OF ARGON AND OXYGEN

Martia Shahsavan
Dept. of Mechanical Engineering
University of Massachusetts Lowell
Lowell, MA, USA

Mohammadrasool Morovatiyan
Dept. of Mechanical Engineering
University of Massachusetts Lowell
Lowell, MA, USA

J. Hunter Mack
Dept. of Mechanical Engineering
University of Massachusetts Lowell
Lowell, MA, USA

ABSTRACT

Natural gas is traditionally considered as a promising fuel in comparison to gasoline due to the potential of lower emissions and significant domestic reserves. These emissions can be further diminished by using noble gases, such as argon, instead of nitrogen as the working fluid in internal combustion engines. Furthermore, the use of argon as the working fluid can increase the thermodynamic efficiency due to its higher specific heat ratio. In comparison to pre-mixed operation, the direct injection of natural gas enables the engine to reach higher compression ratios while avoiding knock. Using argon as the working fluid increases the in-cylinder temperature at top dead center and enables the compression ignition of natural gas. In this numerical study, the combustion quality and ignition behavior of methane injected into a mixture of oxygen and argon has been investigated using a three-dimensional transient model of a constant volume combustion chamber. A dynamic structure large eddy simulation model has been utilized to capture the behavior of the non-premixed turbulent gaseous jet. A reduced mechanism consists of 22-species and 104-reactions were coupled with the CFD solver. The simulation results show that the methane jet ignites at engine-relevant conditions when nitrogen is replaced by argon as the working fluid. Ignition delay times are compared across a variety of operating conditions to show how mixing affects jet development and flame characteristics.

Keywords: Non-premixed Combustion Modeling; Natural Gas; Gaseous Fuels; Noble Gases

NOMENCLATURE

AMR	Adaptive Mesh Refinement
BDC	Bottom Dead Center
CAD	Crank Angle Degree
CFD	Computational Fluid Dynamics
CFL	Courant Friedrichs Lewy
CI	Compression Ignition
CN	Cetane Number
CVCC	Constant Volume Combustion Chamber
d_f	Nozzle diameter
HCCI	Homogeneous Charge Compression Ignition
LES	Large Eddy Simulation
NOx	Oxides of Nitrogen
PISO	Pressure Implicit Split Operator
r	Compression ratio
RCCI	Reactivity Controlled Compression Ignition
RON	Research Octane Number
S	Penetration length
$\tilde{S}$	Normalized penetration length
SI	Spark Ignition
SOR	Successive Over-relaxation
SOx	Oxides of Sulfur
t	Time
$\tilde{t}$	Normalized time
TDC	Top Dead Center
α	Cutoff ratio
γ	Specific heat ratio
η	Ideal thermal efficiency
$\tilde{\rho}$	Density ratio of fuel and working fluid

INTRODUCTION

Natural gas is a fossil fuel composed primarily of methane (more than 90%), other higher alkanes such as propane, and a small percentage of carbon dioxide, nitrogen, helium, and hydrogen sulfide. It is quite abundant in nature, and can be accessed by most of the countries in the world. In the United States, natural gas is one of the main sources of energy supply and electricity production. It is known as the cleanest fossil fuel, which generates less carbon dioxide, NOx, and SOx compared to oil and coal [1]. Due to the abundancy and relatively cleaner essence, natural gas has gained interest in various energy consumption applications including transportation [2].

Recently, natural gas has been extensively used in gas turbines [3] and different types of internal combustion (IC) engines including spark ignition (SI) [4-8], homogeneous charge compression ignition (HCCI) [9-12], reactivity controlled compression ignition (RCCI) [13-15], and as a standalone fuel [16, 17] or blend with other fuels such as diesel [18, 19] and hydrogen [20, 21]. The higher Research Octane number (RON) of natural gas (120-130) enables its utilization at higher compression ratios than gasoline. Moreover, it is cleaner and cheaper than gasoline and diesel. In terms of energy efficiency, natural gas possesses an almost equal efficiency to gasoline, but lower than that of diesel.

Obtaining a higher thermodynamic efficiency can be achieved by running the engine at a higher compression ratio. Methane as a fuel with a higher RON compared to the traditional fuels used in SI engines, is a perfect candidate for this aim. However, the ideal thermodynamic efficiency of the system can be further increased by replacing nitrogen by a noble gas with a higher specific heat ratio such as argon (Equation 1). This hypothesis has been shown by a number of previous studies [22, 23]. Additionally, using argon has the advantage of eliminating NOx emissions due to the avoidance of nitrogen in the combustion chamber [24]. The effect of argon as working fluid instead of nitrogen on hydrogen combustion has also been investigated, and the results indicate that argon can significantly boost the cycle efficiency [25, 26], increase the flame temperature [27, 28], shorten the ignition delay [29, 30], and improve the mixing rate of the injected fuel and the working fluid [31].

$$\eta = 1 - \frac{1}{r^{\gamma-1}}\left(\frac{\alpha^{\gamma}-1}{\gamma(\alpha-1)}\right) \quad (1)$$

Most of the previous studies investigate the use of natural gas in SI engines [32]. Due to the low Cetane Number (CN) of natural gas, it is almost impossible to employ it in CI engines. Even at the highest possible compression ratios in engine-like conditions, direct injection of natural gas into the hot pressurized air does not result in auto-ignition. However, a significant increase in the peak pressure and temperature of the cylinder may enable the natural gas to be auto-ignited. Theoretically, replacing air by a higher specific heat ratio mixture such as argon-oxygen can strongly affect the maximum in-cylinder temperature and pressure at top dead center (TDC).

In this study, the capability of methane, as the main component of natural gas, to be auto-ignited at different operating conditions is assessed using a computational approach. A constant volume combustion chamber (CVCC) filled by argon-oxygen is employed to investigate the non-premixed combustion of methane. For comparison, all the cases are repeated when the chamber is filled by air. Various parameters including temperature history, ignition delay, penetration length, and cone angle of the injected jet are reported. Furthermore, a non-reacting case of a compression ignition engine involving intake compositions of argon-oxygen and nitrogen-oxygen is studied to understand the difference in operating conditions around TDC, where fuel injection typically occurs.

METHODS

A three dimensional transient simulation of methane injection into a constant volume combustion chamber (CVCC) is carried out using CONVERGE, a CFD solver for modeling complex geometries and intricate phenomena such as combustion. Methane is selected as the fuel, since it is the main component of natural gas. The chamber is a cylindrical type with 50 mm length and 20 mm diameter. The length of the chamber is estimated as an average value of the position of the piston at TDC and BDC in common compression-ignition engines. CONVERGE has an advantage of automatic grid generation. After a grid dependency study, the base grid size is set to 0.5 mm, which leads to slightly more than 125,000 cells. Adaptive mesh refinement (AMR) is then employed on velocity and temperature with maximum embedding level of 4 and 3 respectively. The upper limit of total cells in the domain is 2 million. AMR enables the simulation to efficiently resolve the details of the turbulent jet with a relatively coarse mesh at regions where no reactions or spray dispersion exist. Figure 1 shows how AMR splits the cells as the jet propagates in the domain. A varied time step size with a minimum of 1e-7 and maximum of 3e-4 second is used. Courant Friedrichs Lewy number (CFL), which is a necessary condition for convergence, and Mach number automatically adjust the time step. For a total of 2 ms, methane is injected through a 1 mm diameter nozzle into the chamber, which is filled by 21% oxygen and 79% argon. For comparison, all the cases are repeated when argon is replaced by nitrogen.

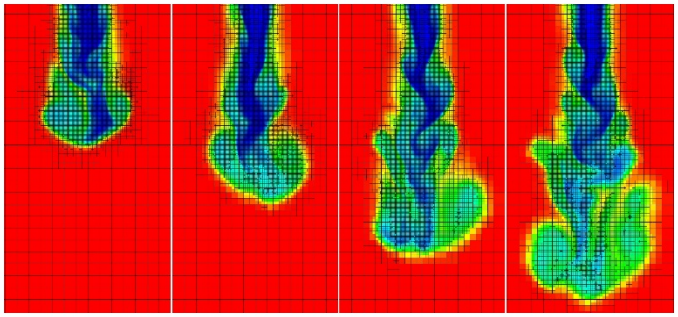

Figure 1. Adaptive Mesh Refinement (AMR) on temperature and velocity. Note that the grid structure changes with the jet progression. This is only a portion of the computational domain.

A CHEMKIN-format reduced mechanism of GRI-MECH, called DRM22, including 22 species and 104 reactions, and the related thermodynamic data are imported into the simulation. For each elementary reaction, a SAGE detailed chemistry solver calculates the reaction rates. For turbulence modeling of the jet, a dynamic structure Large Eddy Simulation (LES) is implemented. It should be noted that a sufficiently fine mesh is required for a desirable LES model to capture the behavior of a turbulent diffusion flame. AMR can drastically reduce the computational cost without a significant loss in solution accuracy. Pressure-velocity coupling in CONVERGE is based on a Pressure Implicit Split Operator (PISO) algorithm. In this simulations, a Successive Over-relaxation (SOR) algorithm is used for momentum, pressure, density, energy, and species equations. For gaseous fuel injection, an average velocity of 100 m/s is assumed, and the flow is modeled downstream of the Mach disk to avoid the intricacy of supersonic flow and shock waves.

In order to investigate the impact of argon as working fluid, and compare it to nitrogen, the chamber is filled by 21% oxygen and 79% argon at different initial temperatures and pressures ranging from 1000 K to 1600 K, and 1 bar to 120 bar. At each case, the temperature history is recorded, and ignition delay, which is the time interval between the injection and the onset of combustion, is calculated. Extrapolation of the steepest slope of the OH, temperature, or pressure curves to the pre-ignition baseline are the most common methods of ignition delay measurement [33]. In this study, the temperature rise is used to calculate the ignition delay.

In addition to ignition delay and flame temperature, fuel propagation is important in the study of non-premixed combustion. Two crucial parameters in jet development studies are penetration length and cone angle. Penetration length is the maximum distance of the jet from the tip of the injector, and the cone angle is the angle of the jet at its largest width. The results of the simulations are exported as images presenting density contour. Then, the image analysis is performed using image processing toolbox of MATLAB. As shown in Figure 2, the grayscale image is used to measure the penetration length and cone angle. The pixel intensity on the centerline of the injector is plotted. The first point where the pixel intensity drops below a certain value, 200 here, represents the tip of the jet, and its distance from the injector tip is reported as penetration length. For cone angle, several filters and thresholds are applied on each image to detect the edge of the jet. First, a binary gradient image with a threshold value of 0.5 is generated using edge function. In order to fill the gaps of the gradient image, line type strel function was used to dilate the image. Then, the imfill function was added to fill the remaining gaps. The next filter is called diamond type strel function, which is used to smoothen the image. Finally, the outline of the image can be obtained by using bwperim function. The longest perpendicular distance of the jet edge from the injection axis is used for cone angle calculation. This approach, rather than using the density provided by the computations, is used to complement experimental results captured using Schlieren imaging techniques.

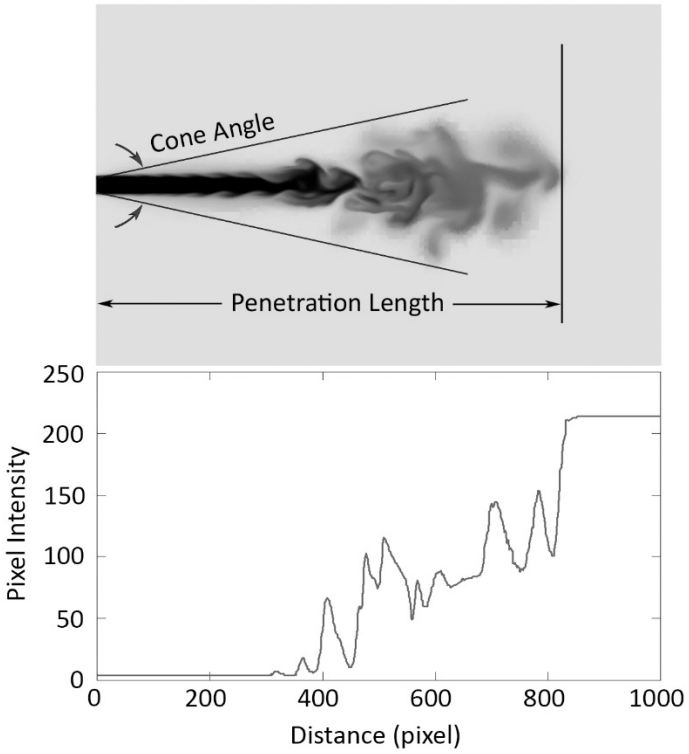

Figure 2. A sample result of the simulation showing density distribution, and calculation of the main parameters of the injected jet: penetration length and cone angle. This is only a portion of the computational domain.

To assess the effect of argon as working fluid on non-premixed combustion of natural gas, the initial temperature and pressure of the chamber should be rationally estimated. The lower specific heat of argon compared to nitrogen should theoretically provide a higher in-cylinder temperature at TDC in compression ignition engines. For this reason, a single bore diesel engine is modeled without injection (non-reacting) in

order to investigate the maximum temperature and pressure history when argon is the working fluid instead of nitrogen. The specifications of the compression ignition engine used in this study are shown in Table 1.

Table 1. Engine specifications

Compression ratio	16.2
Bore	79.5 mm
Stroke	85.0 mm
Connecting rod length	130.0 mm
Engine speed	1500.0 rpm
Intake valve open (IVO)	4 °CA bTDC
Intake valve close (IVC)	44 °CA aBDC
Exhaust valve open (EVO)	56 °CA bBDC
Exhaust valve close (EVC)	0 °CA aTDC

MODEL VALIDATION

In order to assess the reliability of the model, the experimental data of helium injection into air at atmospheric temperature and pressure have been used to validate the measured penetration length and cone angle [34]. A normalization method [35] represented in Equations 2 and 3 allows for comparison of penetration lengths of different fuels at varied operating conditions. In these equations, $\tilde{S}$ and $\tilde{t}$ are the normalized penetration length and time, d_f is the nozzle diameter, $\tilde{\rho}$ is the density ratio of fuel and the working fluid, $\theta/2$ is the half cone angle, U_f is the injection velocity, and a is a constant equal to 0.66.

$$\tilde{S} = \frac{S}{\left(d_f \cdot \tilde{\rho}^{1/2}\right) \Big/ \left(a \cdot \tan(\theta/2)\right)} \tag{2}$$

$$\tilde{t} = \frac{t}{\left(d_f \cdot \tilde{\rho}^{1/2}\right) \Big/ \left(a \cdot \tan(\theta/2) . U_f\right)} \tag{3}$$

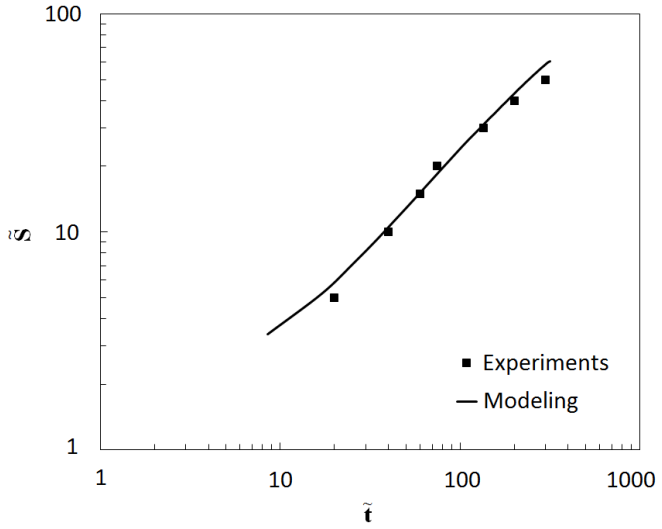

Figure 3. Model validation for normalized penetration length with helium gas injection experiments at ambient pressure and temperature.

As shown in Figure 3, the penetration length results from the modeling are in a satisfactory agreement with the experimental data. The measured half cone angle is 15.8 degrees, which is in an acceptable deviation of the average experimental data (15.4 degrees). Validation of the important parameters of gas jet dispersion enables the model to be reliably used for this numerical study.

RESULTS AND DISCUSSION

The chamber is filled by 21% oxygen and 79% argon at 1 bar and methane is injected through a 1 mm nozzle. For comparison, argon is replaced by nitrogen and the simulation is repeated. Various initial temperatures ranging from 1000 K to 1600 K were examined for both mixtures in order to explore the ignition and flame temperature. The injection duration is 2 ms, and the simulation is continued for 10 ms. At 1000 K, none of the mixtures provide the required conditions for auto-ignition of the methane. Increasing the initial temperature seems to have no effect on auto-ignition of the methane even until 1250 K. At the initial temperature of 1280 K, methane auto-ignites in argon-oxygen mixture after about 9 ms, while no ignition occurs when nitrogen-oxygen is the mixture.

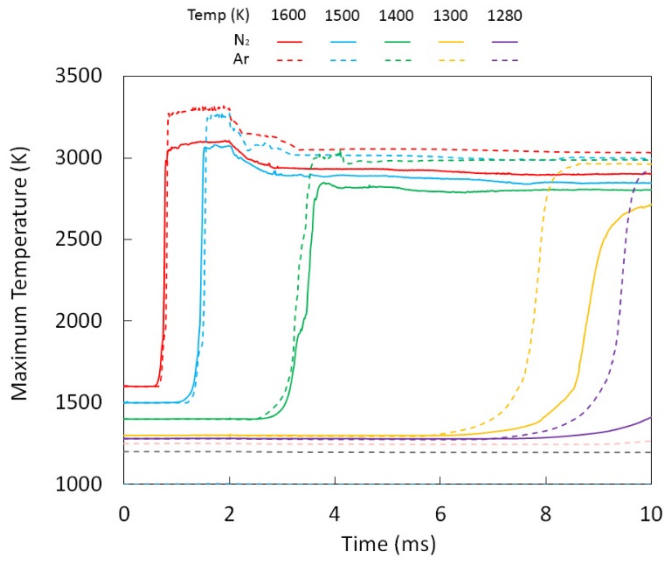

Figure 4. Maximum temperature history at chamber pressure of 1 bar for nitrogen and argon as working fluids and different initial temperatures.

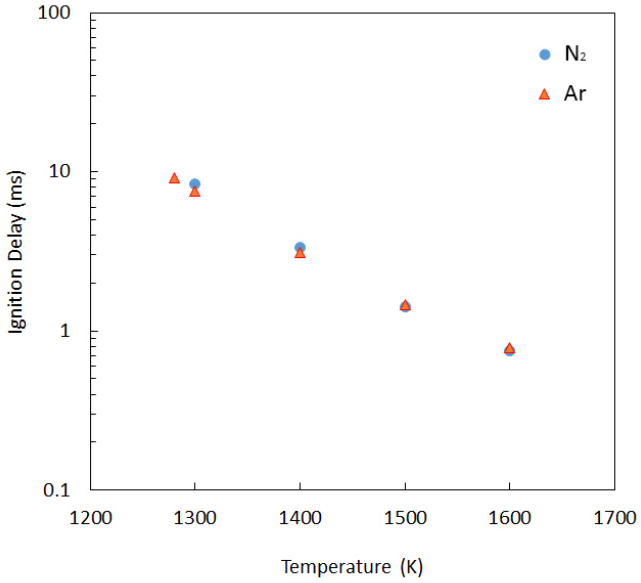

Figure 5. Ignition delay versus temperature for nitrogen and argon as working fluids.

Figure 4 indicates the history of maximum temperature inside the chamber at 1 bar and different initial temperatures. The auto-ignition of methane occurs earlier when the chamber is filled by a mixture at higher temperatures. Moreover, it results in a higher maximum flame temperature. For 1500 K and 1600 K, the ignition delay is less than 2 ms. Therefore, the maximum temperature slightly drops at 2 ms when the injected fuel stream ceases. The ignition timing is more sensitive to the initial temperature when nitrogen is the working fluid, since it leads to even a slightly shorter ignition delay at 1500 K and 1600 K compared to argon. Conversely, the methane ignites quite faster in argon-oxygen compared to nitrogen-oxygen at temperatures 1400 K and below. This shows that nitrogen can compete with argon for the initiation of the fuel ignition when the initial temperature is sufficiently high, whereas it results in a longer ignition delay at lower temperatures. From Figure 5, it is obvious that ignition delay decreases when the chamber temperature increases. At 1600 K, the ignition delay of methane in argon-oxygen is almost an order of magnitude smaller compared to 1280 K.

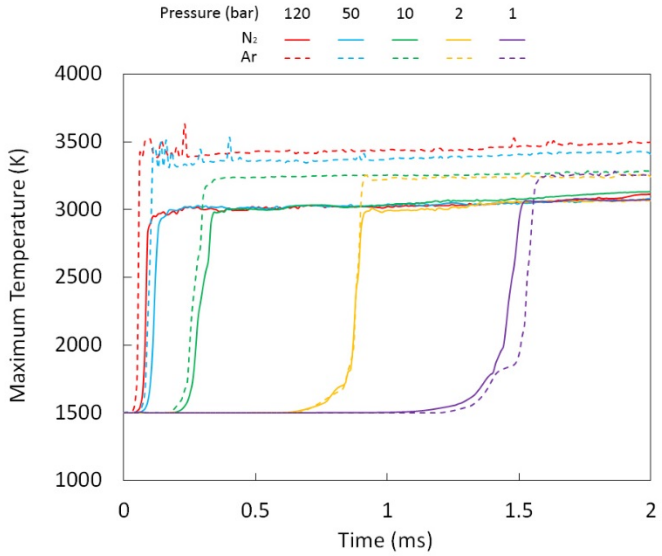

Figure 6. Maximum temperature history at chamber temperature of 1500 K for nitrogen and argon as working fluids and different initial pressures.

To investigate the effect of initial pressure on ignition delay and maximum flame temperature, the chamber is filled by argon-oxygen at 1500 K, and pressure ranging from 1 bar to 120 bar. The same simulations are performed when nitrogen is the primary working fluid instead of argon for comparison. The results in Figure 6 indicate that increasing the initial pressure inside the chamber expedites the ignition. At 1 bar, nitrogen provides a shorter ignition delay for methane compared to argon. At 2 bar, ignition occurs almost at the same time in both working fluids. However, at higher pressures (10, 50, and 120 bar) methane ignites earlier in argon-oxygen compared to its counterpart. This implies that argon performs better in engine-like pressures compared to nitrogen in terms of ignition timing.

Furthermore, the flame temperature of methane is significantly higher in engine-like conditions. Increasing the pressure does not alter the flame temperature when nitrogen is the working fluid. However, it slightly affects the flame temperature in the case of argon-oxygen. This is most probably due to the pressure dependence of the rate constants in the mechanism. At engine-like pressures, the flame temperature of methane slightly increases (about 100 K) when argon is used as the working

fluid. In such cases, the calculated rate constants are higher, which leads to a significantly shorter ignition delay, higher OH concentration, and higher maximum flame temperature consequently. Due to the lower specific heat of argon, the maximum temperature in the domain is larger at all the uniform operating conditions.

Ignition delay versus pressure at a constant temperature of 1500 K is shown in Figure 7. As previously described, increasing the pressure can significantly alter the ignition timing. The ignition delay of methane in argon-oxygen at 1 bar is 1.46 ms, while it is 0.22 ms at 10 bar and 0.05 ms at 120 bar for the same mixture. Additionally, the ignition timing of methane is slightly more pressure sensitive in argon compared to nitrogen.

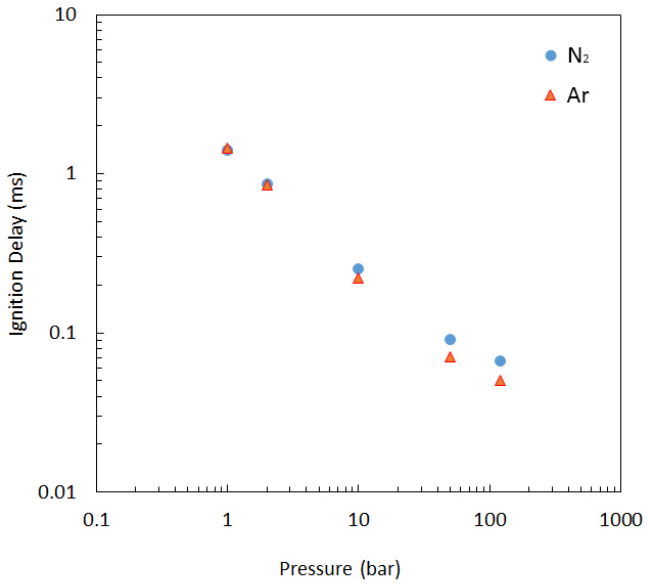

Figure 7. Ignition delay versus pressure at 1500 K for nitrogen and argon as working fluids.

To study the jet shape and fuel propagation in the chamber, penetration length and cone angle are calculated using image processing and the results are presented in Figure 8 and Figure 9 respectively. The operating conditions are initial pressure of 1 bar and initial temperature ranging from 1300 K to 1600 K.

The penetration length and cone angle are almost equal for all cases until 0.3 ms after injection. This can be related to the dominant effect of convection near the injector nozzle, where methane is injected into the chamber at a high velocity, and diffusion effects are not significant. Therefore, the jet shape looks similar at early stages after injection. However, diffusion plays a more important role in the jet dispersion as the methane moves toward the end wall of the chamber. Consequently, the injected fuel behaves differently in terms of distribution at varied operating conditions. The methane jet penetrates more in higher chamber temperatures as a result of lower density of the mixture. At a uniform operating conditions, the injected fuel moves slightly faster in nitrogen-oxygen compared to argon-oxygen. This originates from the lower molecular weight and density of nitrogen. Therefore, the jet shape is more propagated toward the side walls in argon mixture. On average, jet impingement occurs 0.13 ms earlier in nitrogen mixture.

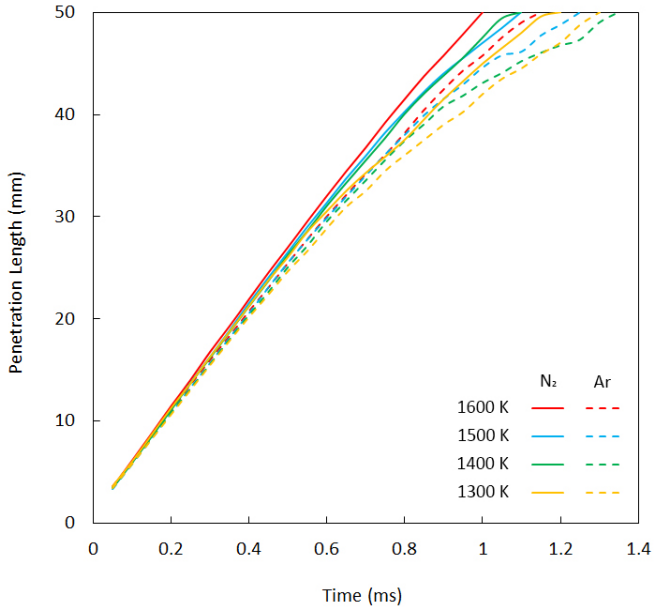

Figure 8. Penetration length versus time at chamber pressure of 1 bar for nitrogen and argon as working fluids and different initial temperatures.

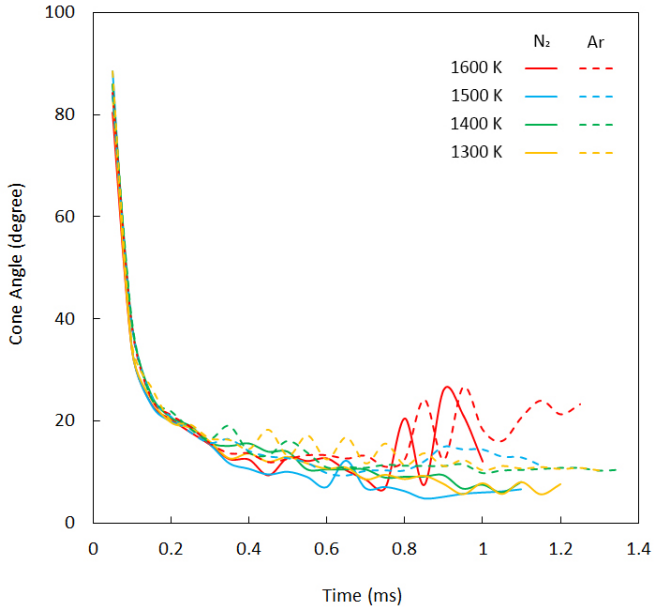

Figure 9. Cone angle versus time at chamber pressure of 1 bar for nitrogen and argon as working fluids and different initial temperatures.

As a result of the previous argument about the jet shape in early stages after the start of injection, the cone angle remains almost constant for all the cases until 0.3 ms. The cone angle results represented in Figure 9 are consistent with the penetration length values. Equal amount of injected fuel causes the jet to have a higher cone angle in the cases that have shorter penetration lengths. Indeed, the injected fuel propagates more in the radial direction when it penetrates less in axial direction. Thus, the methane jet shows a higher cone angle in argon compared to nitrogen. It can be interpreted that the mixture entrainment into the fuel is higher when nitrogen is replaced by argon. The fluctuations in the cone angle curves are due to the turbulence and chaotic propagation of the jet. As temperature rises in the chamber, more cone angle variations can be observed. At 1600 K initial temperature, the fluctuations maximize and behave quite different compared to the other cases. According to the ignition delay data at 1 bar shown in Figure 4 and Figure 5, methane jet ignites at 0.75 ms in nitrogen-oxygen, and 0.78 ms in argon-oxygen mixture. At the onset of combustion, radicals are produced and different species including OH, CO, and unsaturated hydrocarbons are generated, consumed and contributed in the chain reactions. This leads to the change in density distribution in the chamber. Therefore, the calculated cone angle fluctuates more.

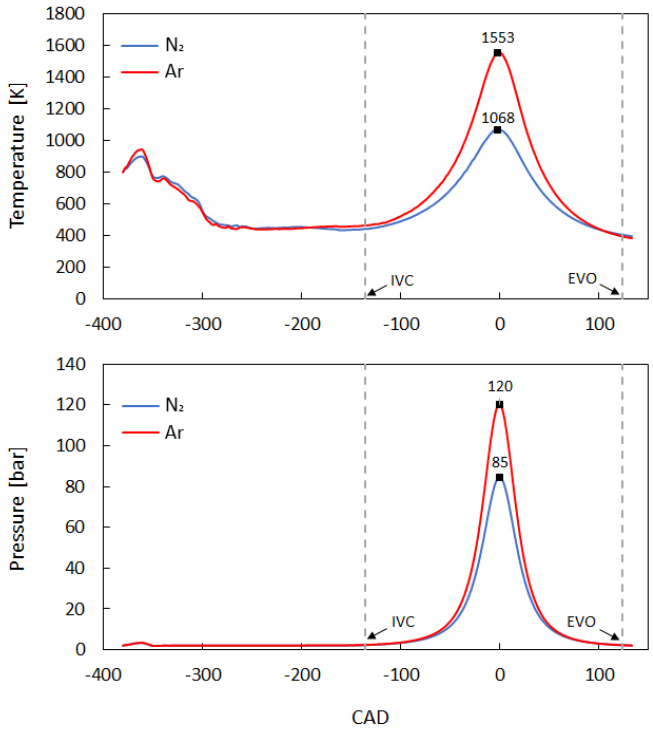

Figure 10. In-cylinder temperature and pressure history for 79% nitrogen and argon in combination with 21% oxygen.

The comparison of the jet behavior, ignition timing and flame temperature in argon and nitrogen mixture at uniform operating conditions were investigated. However, the real operating conditions in compression ignition engines may be different when nitrogen is replaced by argon. In order to determine the initial temperature and pressure of the mixture at the injection event, a non-reacting case in a diesel engine is modeled. Figure 10 shows the result of this simulation.

At TDC, the in-cylinder temperature and pressure are 1068 K and 85 bar respectively in the nitrogen mixture case. However, when argon is the working fluid, the in-cylinder temperature and pressure increase significantly to 1553 K and 120 bar respectively. This is a huge difference is operating conditions since both temperature and pressure are boosted 50% more when nitrogen is simply replaced by argon. CVCC Simulation results indicate that methane does not auto-ignite in nitrogen-oxygen mixture at 1000 K even when the pressure is 85 bar. On the other hand, direct injection of methane into argon-oxygen mixture at 1500 K and 120 bar auto-ignites at 0.05 ms.

CONCLUSIONS

This work represents the effect of argon as working fluid on non-premixed combustion of natural gas. A three dimensional transient simulation is used to study the capability of natural gas to auto-ignite at different media and operating conditions.

The following are the outcomes of this study:

- The maximum temperature and pressure at TDC is about 50% higher when argon is used in combination with oxygen instead of air. The lower specific heat of argon provides a significantly hotter and more pressurized medium for auto-ignition of natural gas.
- Increasing the initial temperature expedites the onset of combustion. At P = 1 bar, the ignition delay of methane in argon-oxygen decreases almost an order of magnitude when the initial temperature of the chamber changes from 1280 K to 1600 K.
- Increasing the initial pressure leads to a shorter ignition delay. At T = 1500 K and P = 1 bar, methane auto-ignites in 1.46 ms in argon-oxygen. While, it decreases to 0.25 ms at 10 bar, and 0.05 ms at 120 bar.
- The maximum temperature in the chamber is higher when nitrogen is replaced by argon at all identical operating conditions.
- Methane jet shape is different in argon-oxygen when compared to nitrogen-oxygen. It penetrates slightly less and generates a larger cone angle in argon mixture. Due to the higher density of argon, the injected fuel propagates more toward the side walls (in radial direction) which provides a more entrainment and mixing. Additionally, the ignition causes fluctuations in cone angle.

- Replacing nitrogen by argon can provide the essential operating conditions for auto-ignition of natural gas. Methane does not auto-ignite at engine-like conditions in TDC (1000 K, 85 bar). However, using argon instead of nitrogen increases the in-cylinder temperature and pressure at TDC (1500 K, 120 bar), which leads to the auto-ignition of methane at 0.05 ms. Additionally, argon replacement can eliminate NOx emissions in the exhaust port.

ACKNOWLEDGMENTS

This research was funded by the University of Massachusetts Lowell. The authors would like to acknowledge CONVERGE support team for their guidance on the numerical simulations.

REFERENCES

[1] M. Dresselhaus and I. Thomas, "Alternative energy technologies," *Nature,* vol. 414, no. 6861, p. 332, 2001.

[2] M. P. Hekkert, F. H. Hendriks, A. P. Faaij, and M. L. Neelis, "Natural gas as an alternative to crude oil in automotive fuel chains well-to-wheel analysis and transition strategy development," *Energy policy,* vol. 33, no. 5, pp. 579-594, 2005.

[3] A. Kalantari, E. Sullivan-Lewis, and V. McDonell, "Application of a turbulent jet flame flashback propensity model to a commercial gas turbine combustor," *Journal of Engineering for Gas Turbines and Power,* vol. 139, no. 4, p. 041506, 2017.

[4] A. Javaheri, V. Esfahanian, A. Salavati-Zadeh, and M. Darzi, "Energetic and exergetic analyses of a variable compression ratio spark ignition gas engine," *Energy Conversion and Management,* vol. 88, pp. 739-748, 2014.

[5] M. Morovatiyan, M. Shahsavan, and J. H. Mack, "Development of a Constant Volume Combustion Chamber for Material Synthesis," in *Eastern States Section of the Combustion Institute Spring Technical Meeting*, State College, PA, 2018.

[6] D. R. Johnson, R. Heltzel, A. C. Nix, N. Clark, and M. Darzi, "Greenhouse gas emissions and fuel efficiency of in-use high horsepower diesel, dual fuel, and natural gas engines for unconventional well development," *Applied Energy,* vol. 206, pp. 739-750, 2017.

[7] S. Szwaja *et al.*, "Influence of exhaust residuals on combustion phases, exhaust toxic emission and fuel consumption from a natural gas fueled spark-ignition engine," *Energy Conversion and Management,* vol. 165, pp. 440-446, 2018.

[8] M. R. Morovatiyan and V. Hosseini, "Development of a 3D CFD model to analyze gas exchange process into intake manifold of an iVVT engine," *The Journal of Engine Research,* vol. 36, no. 36, pp. 51-60, 2014.

[9] D. Flowers, S. Aceves, C. Westbrook, J. Smith, and R. Dibble, "Detailed chemical kinetic simulation of natural gas HCCI combustion: gas composition effects and investigation of control strategies," *Journal of engineering for gas turbines and power,* vol. 123, no. 2, pp. 433-439, 2001.

[10] Z. M. Hammond, J. H. Mack, and R. W. Dibble, "Effect of hydrogen peroxide addition to methane fueled homogeneous charge compression ignition engines through numerical simulations," *International Journal of Engine Research,* vol. 17, no. 2, pp. 209-220, 2016.

[11] A. Y. Nobakht, R. K. Saray, and A. Rahimi, "A parametric study on natural gas fueled HCCI combustion engine using a multi-zone combustion model," *Fuel,* vol. 90, no. 4, pp. 1508-1514, 2011.

[12] M. Shahsavan and J. H. Mack, "Numerical study of a boosted HCCI engine fueled with n-butanol and isobutanol," *Energy Conversion and Management,* vol. 157, pp. 28-40, 2018.

[13] E. Ansari, K. Poorghasemi, B. K. Irdmousa, M. Shahbakhti, and J. Naber, "Efficiency and Emissions Mapping of a Light Duty Diesel-Natural Gas Engine Operating in Conventional Diesel and RCCI Modes," SAE Technical Paper 0148-7191, 2016.

[14] A. Paykani, A.-H. Kakaee, P. Rahnama, and R. D. Reitz, "Effects of diesel injection strategy on natural gas/diesel reactivity controlled compression ignition combustion," *Energy,* vol. 90, pp. 814-826, 2015.

[15] K. Poorghasemi, R. K. Saray, E. Ansari, B. K. Irdmousa, M. Shahbakhti, and J. D. Naber, "Effect of diesel injection strategies on natural gas/diesel RCCI combustion characteristics in a light duty diesel engine," *Applied Energy,* vol. 199, pp. 430-446, 2017.

[16] D. Johnson, M. Darzi, C. Ulishney, M. Bade, and N. Zamani, "Methods to Improve Combustion Stability, Efficiency, and Power Density of a Small, Port-Injected, Spark-Ignited, Two-Stroke Natural Gas Engine," in *ASME 2017 Internal Combustion Engine Division Fall Technical Conference*, 2017, pp. V002T07A008-V002T07A008: American Society of Mechanical Engineers.

[17] A.-H. Kakaee, A. Paykani, and M. Ghajar, "The influence of fuel composition on the combustion and emission characteristics of natural gas fueled engines," *Renewable and Sustainable Energy Reviews,* vol. 38, pp. 64-78, 2014.

[18] A. Carlucci, A. d. de Risi, D. Laforgia, and F. Naccarato, "Experimental investigation and combustion analysis of a direct injection dual-fuel diesel–natural gas engine," *Energy,* vol. 33, no. 2, pp. 256-263, 2008.

[19] A.-H. Kakaee, P. Jafari, and A. Paykani, "Numerical Study of Natural Gas/Diesel Reactivity Controlled Compression Ignition Combustion with Large Eddy

Simulation and Reynolds-Averaged Navier–Stokes Model," *Fluids,* vol. 3, no. 2, p. 24, 2018.

[20] B. Afkhami, A. Kakaee, and K. Pouyan, "Studying engine cold start characteristics at low temperatures for CNG and HCNG by investigating low-temperature oxidation," *Energy conversion and management,* vol. 64, pp. 122-128, 2012.

[21] F. Ma, Y. Wang, H. Liu, Y. Li, J. Wang, and S. Zhao, "Experimental study on thermal efficiency and emission characteristics of a lean burn hydrogen enriched natural gas engine," *International Journal of Hydrogen Energy,* vol. 32, no. 18, pp. 5067-5075, 2007.

[22] N. J. Killingsworth, V. H. Rapp, D. L. Flowers, S. M. Aceves, J.-Y. Chen, and R. Dibble, "Increased efficiency in SI engine with air replaced by oxygen in argon mixture," *Proceedings of the Combustion Institute,* vol. 33, no. 2, pp. 3141-3149, 2011.

[23] R. Kuroki, A. Kato, E. Kamiyama, and D. Sawada, "Study of high efficiency zero-emission argon circulated hydrogen engine," SAE Technical Paper 0148-7191, 2010.

[24] H. A. Moneib, M. Abdelaal, M. Y. Selim, and O. A. Abdallah, "NOx emission control in SI engine by adding argon inert gas to intake mixture," *Energy Conversion and Management,* vol. 50, no. 11, pp. 2699-2708, 2009.

[25] M. Sierra-Aznar *et al.*, "Working fluid replacement in gaseous direct-injection internal combustion engines: A fundamental and applied experimental investigation," in *10th US National Combustion Meeting*, College Park, MD, 2017.

[26] N. M. Hafiz, M. R. A. Mansor, and W. M. F. Wan Mahmood, "Simulation of the combustion process for a CI hydrogen engine in an argon-oxygen atmosphere," *International Journal of Hydrogen Energy,* vol. 43, no. 24, pp. 11286-11297, 2018.

[27] M. Shahsavan and J. Mack, "The effect of heavy working fluids on hydrogen combustion," in *10th US National Combustion Meeting*, College Park, MD, 2017.

[28] M. R. A. Mansor and M. Shioji, "Investigation of the combustion process of hydrogen jets under argon-circulated hydrogen-engine conditions," *Combustion and Flame,* vol. 173, pp. 245-257, 2016.

[29] M. Shahsavan, M. Morovatiyan, and J. H. Mack, "The Influence of Mixedness on Ignition for Hydrogen Direct Injection in a Constant Volume Combustion Chamber," in *Eastern States Section of the Combustion Institute Spring Technical Meeting*, State College, PA, 2018.

[30] M. Shahsavan, M. Morovatiyan, and J. H. Mack, "A numerical investigation of hydrogen injection into noble gas working fluids," *International Journal of Hydrogen Energy,* vol. 43, no. 29, pp. 13575-13582, 2018.

[31] M. Shahsavan and J. H. Mack, "Mixedness Measurement in Gaseous Jet Injection," in *American Society for Engineering Education Northeast Section (ASEE-NE)*, Lowell, MA, 2017.

[32] H. M. Cho and B.-Q. He, "Spark ignition natural gas engines—A review," *Energy conversion and management,* vol. 48, no. 2, pp. 608-618, 2007.

[33] S. S. Vasu, D. F. Davidson, and R. K. Hanson, "Jet fuel ignition delay times: Shock tube experiments over wide conditions and surrogate model predictions," *Combustion and Flame,* vol. 152, no. 1, pp. 125-143, 2008.

[34] M. J. Borz, Y. Kim, and J. O'Connor, "The Effects of Injection Timing and Duration on Jet Penetration and Mixing in Multiple-Injection Schedules," SAE Technical Paper 0148-7191, 2016.

[35] J. D. Naber and D. L. Siebers, "Effects of gas density and vaporization on penetration and dispersion of diesel sprays," SAE technical paper 0148-7191, 1996.